J. of Cardiovasc. Trans. Res. (2014) 7:719–736
DOI 10.1007/s12265-014-9590-4

Imaging of Oxidation-Specific Epitopes with Targeted Nanoparticles to Detect High-Risk Atherosclerotic Lesions: Progress and Future Directions

Karen Briley-Saebo · Calvin Yeang · Joseph L. Witztum · Sotirios Tsimikas

Received: 3 June 2014 / Accepted: 12 September 2014 / Published online: 9 October 2014

Abstract Oxidation-specific epitopes (OSE) within developing atherosclerotic lesions are key antigens that drive innate and adaptive immune responses in atherosclerosis, leading to chronic inflammation. Oxidized phospholipids and malondialdehyde-lysine epitopes are well-characterized OSE present in human atherosclerotic lesions, particularly in pathologically defined vulnerable plaques. Using murine and human OSE-specific antibodies as targeting agents, we have developed radionuclide and magnetic resonance based nanoparticles, containing gadolinium, manganese or lipid-coated ultrasmall superparamagnetic iron oxide, to non-invasively image OSE within experimental atherosclerotic lesions. These methods quantitate plaque burden, allow detection of lesion progression and regression, plaque stabilization, and accumulation of OSE within macrophage-rich areas of the artery wall, suggesting they detect the most active lesions. Future studies will focus on using "natural" antibodies, lipopeptides, and mimotopes for imaging applications. These approaches should enhance the clinical translation of this technique to image, monitor, evaluate efficacy of novel therapeutic agents, and guide optimal therapy of high-risk atherosclerotic lesions.

Keywords Imaging · Oxidation · Atherosclerosis · Magnetic resonance · Inflammation

Associate Editor Paul J. R. Barton oversaw the review of this article.

K. Briley-Saebo
Department of Basic Science and Craniofacial Biology, New York University, New York, NY, USA

C. Yeang · J. L. Witztum · S. Tsimikas (✉)
Division of Cardiovascular Medicine, University of California San Diego, BSB-1080, La Jolla, CA 92093-0682, USA
e-mail: stsimikas@ucsd.edu

Introduction

The transition of silent atherosclerotic lesions into clinical events is variable and depends on anatomical factors such as plaque burden, location, and functional factors such as hemodynamic parameters and extent of plaque inflammation. A variety of invasive and non-invasive imaging modalities are available to measure the extent of atherosclerosis and predict clinical events or need for revascularization. However, there is often a clinical disconnect between quantitating plaque burden and predicting clinical events, as illustrated by the fact that most myocardial infarctions are difficult to predict based on either clinical assessment or current imaging techniques [1, 2].

It has been well documented that enhanced oxidative stress, leading to generation of oxidized low-density lipoprotein (OxLDL), plays a key role in the initiation, progression and destabilization of atherosclerotic lesions [3–8]. Hypercholesterolemia leads to overproduction of reactive oxygen species (ROS) and upregulation of pro-oxidant enzymes in the vessel wall [9]. ROS generates OxLDL, thereby producing a variety of pro-atherogenic and pro-inflammatory oxidation-specific epitopes (OSE) [10]. OSE are key antigens in the vessel wall that lead to activation of both innate and adaptive immunity, leading to pro-inflammatory responses that promote atherogenesis, but also immune antibody responses that appear to serve protective functions as well [4, 5].

The correlation between the presence of OSE, such as oxidized phospholipids (OxPL) and malondialdehyde (MDA) epitopes, and plaque progression has been demonstrated using direct extraction of modified LDL from the vessel wall [11, 12] and by immunostaining studies in mice, rabbits, monkeys and humans [11, 13–31]. These studies document the strong presence of oxidized lipids in early and intermediate lesions in animal models and evidence of strong expression of OSEs in different stages of plaque progression and plaque rupture in humans with sudden cardiac death [27]. They also demonstrate the prominent presence of

apolipoprotein(a) [apo(a)], a component of lipoprotein (a) [Lp(a)], in the same lesions. This is relevant because we have shown that OxPL are present on Lp(a), which is the primary lipoprotein carrier of OxPL in human plasma [32, 33]. Recent data have shown that Lp(a) is a causal mediator of CVD [34] and aortic valve calcification and stenosis [35–37].

One effect of this pro-inflammatory cascade is the production of immune effector proteins, such as innate natural antibodies (NAbs) and adaptive acquired antibodies to OSE by activated B-1 and B-2 cells respectively [3]. Pre-clinical and clinical studies have demonstrated that innate IgM NAbs to OSEs are atheroprotective [38–40]. A direct correlation between higher levels of OSE-specific IgM at baseline and a reduced risk of subsequent anatomical cardiovascular disease (CVD) and CVD clinical events has been reported [41–43].

Our laboratory has taken advantage of the immunogenicity of OSEs to generate, characterize and evaluate murine and human monoclonal Abs to OSE as targeted molecular imaging agents. The aim of this review is to summarize the role of OSE in atherogenesis, to describe how the innate immune system interacts with OSE to generate OSE-directed NAbs and how these can then be utilized for imaging OSE, and finally to highlight future approaches in translating imaging of OSE to patients. In this review, we will summarize the work targeting OSE in imaging applications. The reader is referred to recent reviews focusing on various molecular imaging modalities to detect high-risk plagues [44–47].

The Role of Oxidation-Specific Epitopes in Atherogenesis

It is now widely accepted that atherosclerosis is a chronic inflammatory disease [48, 49] and that profound innate and adaptive immune responses to OSE play central roles in atherogenesis (reviewed in detail [5, 6, 8, 9, 48]). Oxidation of lipoproteins does not result in a single, defined molecular species, but instead generates a variety of OSE, such as OxPL and MDA-lysine epitopes [5, 50–52]. OSE are biologically active and pro-inflammatory by upregulating adhesion molecules to attract monocytes into the vessel wall, inducing pro-inflammatory gene expression and cytokine responses, and promoting macrophage retention, cytotoxicity, and apoptosis [5, 53]. OSE are pro-atherogenic by mediating the unregulated uptake of OxLDL into macrophages through scavenger receptors (MSR) thereby generating activated macrophage foam cells. Patients presenting with acute coronary syndromes (ACS) have significantly elevated levels of OxPL on apoB-containing lipoproteins (OxPL/apoB), which correlate with the content of OxPL in coronary atherectomy specimens (70-fold greater presence in plaques than plasma) and the severity of disease presentation [27, 54–57].

OSE are potent immunogens and activate T-cells and B-cells resulting in the generation of OSE-Abs [11, 58, 59]. OSE are ubiquitous in atherosclerotic lesions and represent a class of danger-associated molecular patterns (DAMPs), which we postulate has led to the natural selection of multiple innate pattern recognition receptors (PRRs) targeting such OSE (Fig. 1) [3]. Positive selection during evolution has preserved and amplified multiple PRRs that recognize common OSE, which are common on many modified-self structures. Furthermore, OSE share molecular or immunological identity with common epitopes on microbial pathogens. Cellular PRRs include MSR and toll-like receptors (TLRs) on macrophages, and soluble PPRs include NAbs and innate proteins such as C-reactive protein (CRP), other pentraxins, and the family of complement proteins [60]. Oxidation of surface membrane phospholipids in LDL generates OxPL when LDL is oxidized, and similarly, cells undergoing apoptosis generate ROS that lead to the oxidation of OxPL on their cell surfaces. In both settings, there is an altered conformation of the phosphocholine (PC) head group of PC-containing phospholipids, yielding an "exposed" PC epitope, which is then recognized by MSR (CD-36 and SR-B1), NAbs (E06 and T15 as described below), and CRP [61, 62]. Because innate immunity utilizes preformed PRR to mediate responses, it is believed that PRR are selected and conserved by natural selection. Why then would there be innate PRRs directed to OSE? Apoptotic cells become pro-inflammatory and immunogenic if not promptly cleared [63]. We therefore postulate that PC-specific PRRs were selected to clear apoptotic cells from developing or regenerating tissues. Recognition by the same PRRs of the PC epitope present on the capsular polysaccharide (not part of a phospholipid) of many Gram(+) bacteria (e.g., *S. pneumoniae*) provided additional positive selection of such PC-specific PRRs, and probably helped to select additional strong pro-inflammatory components to these PRR-dependent responses. Subsequent findings that many OSE-NAbs secreted from OxLDL-specific B-1 cell lines bind to OSE, block uptake of OxLDL by macrophages, recognize apoptotic cells, and are deposited in atherosclerotic lesions suggests a new role of innate immunity and PRRs in inflammation and atherosclerosis [5, 64].

Immunogenicity of Modified Low Density Lipoproteins and Generation of Antibodies to Oxidation-Specific Epitopes

Immunization of mice with murine OxLDL and MDA-LDL led to the cloning of a variety of "oxidation-specific" monoclonal antibodies (MAbs), which were then used to provide crucial evidence that OxLDL was formed in atherosclerotic lesions in vivo in animals and humans. In turn, it was shown that rabbits, mice, and humans possessed titers of such antibodies to OSE and that these were bound to OxLDL in lesions as part of immune complexes [13, 14, 65]. LDL eluted from the arteries of humans contained such OSE and had all the other physical and biological properties of OxLDL generated

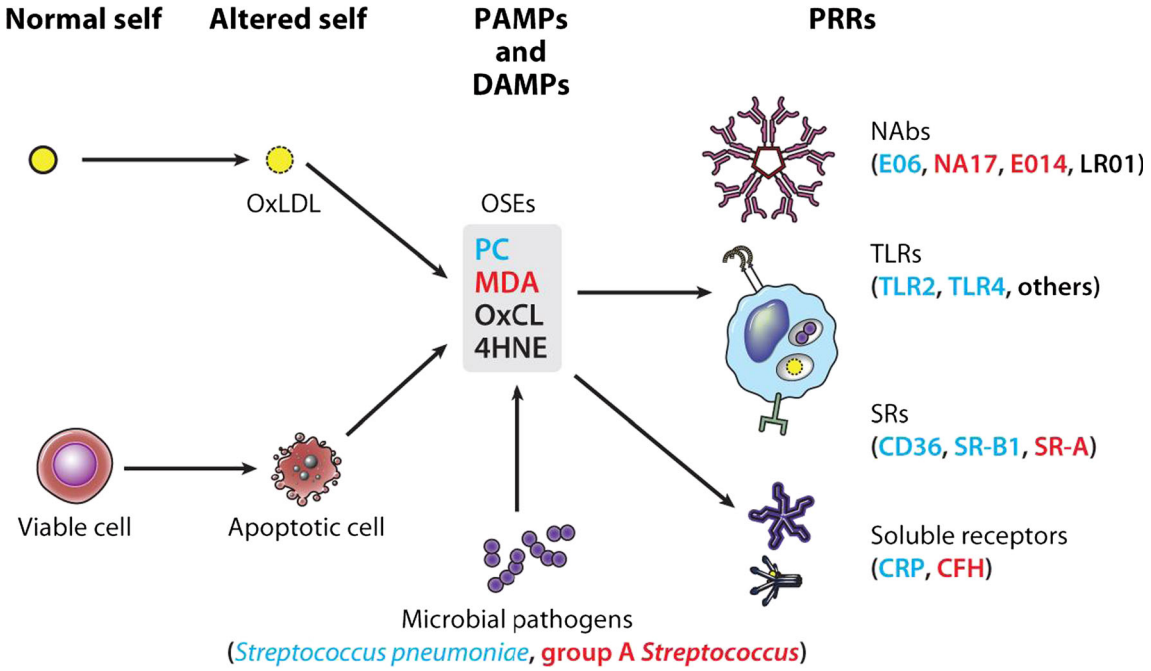

Fig. 1 Summary of oxidation-specific epitopes (OSEs) as major antigens of innate immunity. Oxidation-induced changes in normal self-molecules generate OSEs that are recognized as damage-associated molecular patterns (DAMPs) by the innate immune system. OSEs are also found on apoptotic cells and on microbes (or molecular mimics), where they serve as pathogen-associated molecular patterns (PAMPs). Oxidation of low-density lipoprotein (LDL), which occurs in atherosclerotic lesions, generates several OSEs, such as exposed phosphocholine (PC), malondialdehyde (MDA), oxidized cardiolipin (OxCL), and 4-hydroxynonenal (4HNE). These DAMPs are recognized by various pattern recognition receptors (PRRs) of the innate immune system. For example, PC on OxLDL, apoptotic cells, and *Streptococcus pneumoniae* is recognized by the innate immunoglobulin M (IgM) natural antibody (NAb) E06, the scavenger receptors (SRs) CD36 and SR-B1, and the pentraxin C-reactive protein (CRP). MDA is recognized by the NAbs E014 and NA17, and by SR-A and complement factor H (CFH). An MDA mimic recognized by E014 is found on group A *Streptococcus*. These OSEs and others are present in atherosclerotic lesions and act as major antigens stimulating innate and adaptive responses that affect the progression of vascular disease. Abbreviation: *TLRs* toll-like receptors. Reprinted with permission from Witztum and Lichtman [3]

in vitro, including the important property of being recognized by MSR [11, 12, 65–67]. These data firmly established the presence of OxLDL in atherosclerotic lesions. The observation that high-titered antibodies to OxLDL existed in non-immunized cholesterol-fed apoE$^{-/-}$ mice prompted us to generate hybridomas to OxLDL using their splenic cells [17, 58, 68]. The resulting panels of MAbs (termed E0) were all IgM isotype and were bound to both the lipid and the protein moieties of OxLDL [14], suggesting that they bound to oxidized lipids, which were also covalently bound to apoB. Among a panel of 8 IgM that bound to OxLDL, all had identical V_H/V_L variable region genes that were "germline" rearrangements typical of true NAbs, and all were identical to each other and to the T15 idiotype, an IgA NAb first described 30 years earlier [17].

Oxidation-Specific Epitopes are Present in Vulnerable and Ruptured Human Coronary and Carotid Plaques

In recent studies [27, 30, 31], we demonstrated that presence of OSE in human coronary and carotid arteries, using a variety of OSE MAbs, in lesions ranging from early intimal xanthomas to ruptured plaques in patients with sudden death or undergoing carotid endarterectomy. Figure 2 shows immunostaining of OSE in a human coronary thin cap fibroatheroma (TFCA), a precursor to plaque rupture, and a ruptured plaque. These lesions contain a necrotic core and a cluster of macrophages (brown/black stain) within the fibrous cap. Strong staining is noted for OxPL within the fibrous cap, including macrophages, and necrotic core. Advanced MDA-like epitopes detected by the fully human MAb IK17 are intense in the less lytic areas of the necrotic core. These studies demonstrated that OxPL and IK17 epitopes were most specifically associated with unstable and ruptured coronary plaques, as well as advanced carotid lesions derived following carotid endarterectomy [27]. Using mass spectroscopy, we have recently shown the presence of a variety of OxPL, such as 1-palmitoyl-2-oxovaleroyl-sn-glycero-3-phosphorylcholine (POVPC) and oxidized cholesteryl esters, in the filters of distal protection devices used to trap embolized materials from patients undergoing carotid and peripheral interventions [30, 31]. These data confirm the immunochemical data and definitively demonstrate the presence of pro-inflammatory OSE in late-stage vulnerable plaques of symptomatic patients.

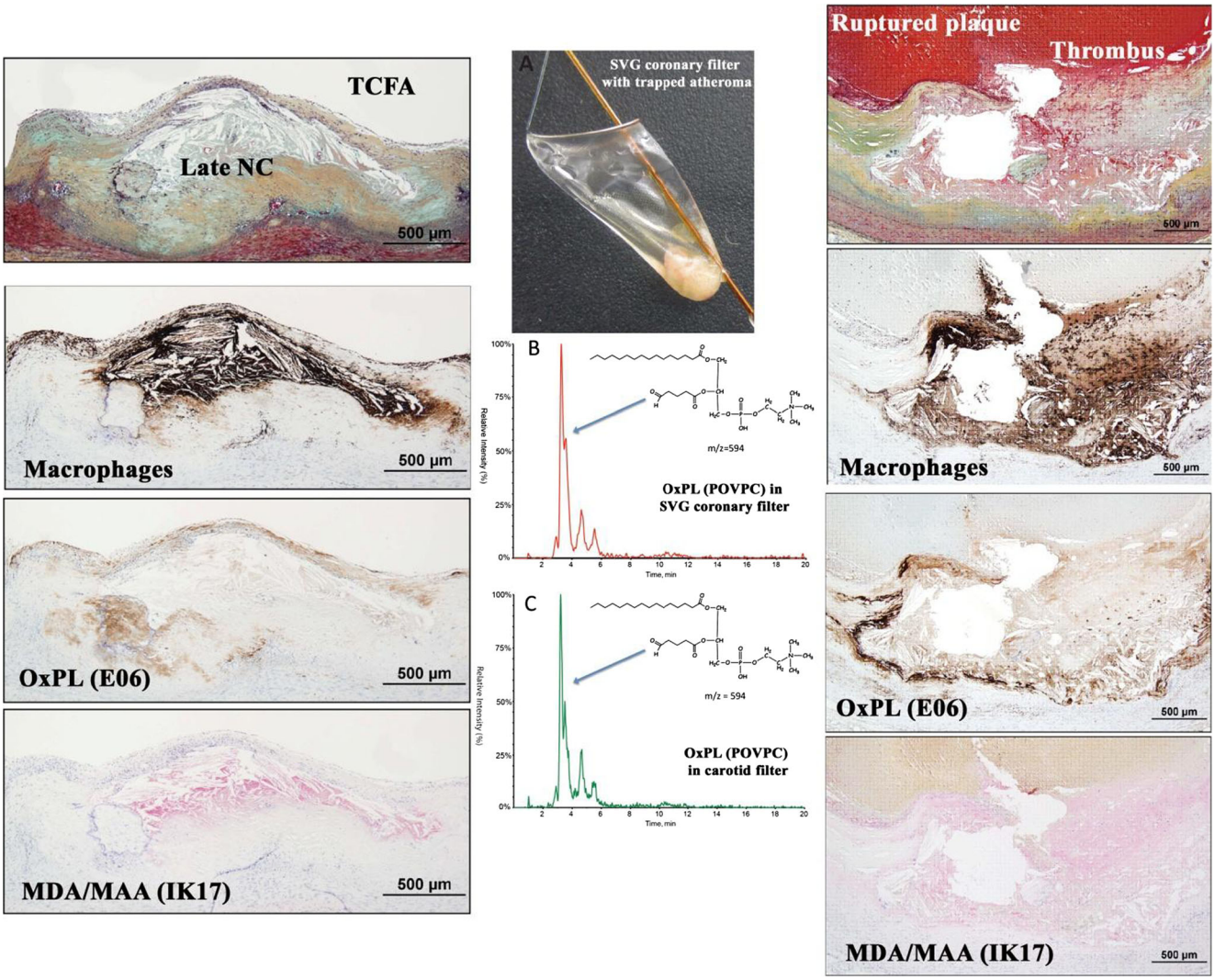

Fig. 2 The presence of macrophages and oxidation-specific epitopes in thin cap fibroatheroma (TCFA, *left panels*) and ruptured coronary plaques (*right panels*) detected by immunohistochemistry and coronary and carotid distal protection devices (*middle panels*) detected by LC-MS/MS. *POVPC*=1-palmitoyl-2-(5′-oxo-valeroyl)-sn-glycero-3-phosphocholine, *NC*=necrotic core, *OxPL*=oxidized phospholipids, *MDA*=malondialdehyde, *MAA*=malondialdehyde acetylaldehyde, *SVG*=saphenous vein graft. Reprinted with permission from van Dijk et al. [27]

Oxidation-Specific Biomarkers Predict Cardiovascular Events in Humans and Oxidation-Specific Antibodies Slow Progression of Atherosclerosis in Mice

The concept of biotheranostics, as previously described [69, 70], relates to the potential of linking biomarker assays, therapeutic applications, and diagnostic imaging thematically around a clinically relevant target that is causal in a disease state. The target is the OSE present either in the circulation or in the vessel wall, and the targeting agents directed to OSE can be used for in vitro ELISA to detect circulating antigens, or coupled with imaging probes in detecting the presence and quantity of OSE present in the artery wall, or used directly as therapeutic agents in neutralizing pro-inflammatory and pro-atherogenic effects of OSE, as briefly described below.

Using E06, we have developed an ELISA to detect OxPL on human apoB (OxPL/apoB) in plasma, and used this to analyze plasma of established epidemiological and intervention studies encompassing over 12,000 patients and nearly 18,000 blood samples (reviewed in Taleb et al.[71] and Leibundgut et al.[69]). OxPL/apoB levels are elevated in patients with ACS[57] and following percutaneous coronary intervention (PCI)[72], predict the progression of femoral/carotid [73] and coronary artery disease (CAD) [74], predict death, myocardial infarction and stroke in unselected populations followed prospectively [43, 75, 76], and reclassify ~30 % of patients to lower or higher risk categories based on clinical criteria and Framingham risk score [43]. In clinical applications, the OxPL/apoB assay may be used to screen patients at high risk for CVD, and then patients may be imaged specifically with OSE targeted nanoparticles to localize the site(s) of disease, which cannot be accomplished with biomarkers.

OSE directed antibodies might also have therapeutic potential. We utilized human MAb IK17-Fab and IK17 single chain Fv fragment (IK17-scFv), which lack immunological properties of intact antibodies other than the ability to inhibit uptake of OxLDL by macrophages, to assess the in vivo importance of MSR-mediated uptake of OxLDL in atherogenesis [22]. Cholesterol-fed $LDLR^{-/-}$ mice were treated with intraperitoneal infusion of IK17-Fab, leading to a 29 % decrease in atherosclerosis progression. However, the effectiveness of the human IK17-Fab was compromised in this study because of the development of neutralizing murine-anti-IK17 Abs. To circumvent the immunogenicity of human IK17 in mice, we expressed IK17-scFv in $LDLR^{-/-}/Rag^{-/-}$ mice (lacking the ability to make Abs due to loss of T and B-cell function) using adenoviral vectors (Adv) and showed that IK17-scFv decreased atherosclerosis progression by 46 %. Importantly, peritoneal macrophages from Adv-IK17-scFv treated mice had decreased lipid accumulation compared to Adv-EGFP mice, suggesting an excess of IK17-scFv prevented foam cell formation by binding to OSE and preventing recognition by MSR.

The IK17 epitopes are strongly present in pathologically-defined vulnerable plaques [27], which suggest a strong rationale that this antibody may have therapeutic potential. However, it is also noted that human lesions are more complex than murine lesions, and the extent of uptake of IK17 in human lesions cannot be fully predicted. Translation of imaging approaches documenting IK17 uptake in human lesions prior to therapeutic studies would provide evidence for targeting IK17 epitopes therapeutically.

Targeted Molecular Imaging Probes

Table 1 summarizes the murine and human OSE autoantibodies, lipopeptides, and mimotopes that have been used or have potential in diagnostic imaging applications. MDA2 (IgG2a type) is a hapten-specific antibody that recognizes MDA-modified proteins. It was generated from a hybridoma derived from mice immunized with homologous murine malondialdehyde (MDA)-modified LDL MDA2 [11, 13, 15, 66]. IK17 Fab, the first fully human OSE monoclonal antibody, was generated from the lymphocytes of a patient with CAD [19] and binds to an advanced MDA-like epitope, malondialdehyde-acetaldehyde (MDA-MAA), which is expressed during extensive oxidative modification and in advanced lesions and vulnerable and ruptured plaques [19, 22–24, 26, 27, 77]. E06, an IgM antibody, was described above [78]. P1 and P2 are MDA-mimotopes, i.e., peptides that appear to have the three dimensional shape of MDA-lysine epitopes. They are linear 12 amino acid peptide and 7-amino acid cyclic peptides, respectively, which were identified by screening peptide phage display libraries with an MAA specific monoclonal antibody. Each peptide represents a consensus sequence from respective linear and cyclic peptide libraries that bound specifically to the murine monoclonal antibody LR04, as well as a human anti-MDA monoclonal antibody, and mimic MDA epitopes on the surface of apoptotic cells [79]. Table 2 summarizes the primary imaging studies targeting OSE with selected studies being described below.

Radionuclide Imaging Studies

For nuclear imaging techniques such as SPECT and PET, probe design is focused on specificity, pharmacokinetics, biodistribution, and radioactive tracer half-life. In vivo imaging must be performed after the antibody or peptide has been cleared from the circulation, or from the nearby tissue, so that the background signal from blood or other tissue (such as lymph) does not interfere with the signal from the arterial wall. Pre-clinical studies using ^{125}I-MDA2 and ^{99m}Tc-MDA2 were performed in atherosclerotic mice and rabbits and imaging was performed 6–24 h after intravenous injection of the radiolabeled antibody [15, 16, 19]. Accumulation of ^{125}I-MDA2 in atherosclerotic lesions was confirmed by autoradiography, ex vivo imaging, lipid staining and immunohistochemistry and the uptake of ^{125}I-MDA2 was highest in the aorta and was directly proportional to plaque burden [16]. Indeed, studies using ^{99m}Tc-MDA2 were also performed in rabbits with diet-induced atherosclerosis, which generates lipid rich lesions, and the results from these studies confirm the selective ability of ^{99m}Tc-MDA2 to detect lipid-rich, OSE-rich plaques [15]

The nuclear imaging approach also provided insights into changes in OSE during plaque progression and regression (induced by dietary changes) in mice, rabbits, and monkeys [16, 18, 20, 21]. It was observed that during plaque progression, OSE accumulation in the arterial wall was proportional to plaque burden (Fig. 3). During regression, many of the lesions were unchanged with respect to size. There was, however, evidence of significant loss of OSE and macrophages in the vessel wall, along with substantial gain in smooth muscle cells and collagen [20]. The loss of OxPL in the vessel wall was also marked by an increase in circulating OxPL/apoB [21], suggesting a flux of OxPL to the circulation where it was bound by apoB lipoproteins. These data are also consistent with human carotid plaques showing loss of the OSE following treatment with pravastatin for 3 months [80]. Interestingly, aged Watanabe heritable hyperlipidemic rabbits were shown to develop fibrotic lesions that exhibited limited ^{125}I-MDA2 uptake [16, 20]. This model may be viewed as a clinical equivalent to obstructive, heavily calcified, and fibrotic lesions with reduced OSE content and a lower propensity to rupture [81]. Overall, these observations suggest that loss of OSE may occur early in plaque stabilization, prior to

Table 1 Properties of murine and human OSE autoantibodies and peptides in imaging applications

Antibody	Source	Epitopes bound	Conjugated labels
MDA2	Murine monoclonal IgG2a	MDA-LDL	^{125}I, ^{99}Tc
		MDA-modified proteins	Gd micelles
			Mn micelles
			Mn dendrimers
			LUSPIO micelles
			LSPIO micelles
E06 (whole IgM or scFv)	Murine monoclonal IgM Natural antibody	PC on oxidized phospholipids but not normal phospholipids	Gd micelles
			Mn micelles
			LUSPIO micelles
			LSPIO micelles
IK17 (Fab, scFv)	Human monoclonal IgG Fab	MDA-LDL	Gd micelles
		Copper OxLDL	Mn micelles
			LUSPIO micelles
			LSPIO micelles
Mimotope	Characteristic	Epitopes mimicked	Antibodies bound
P1	12-mer linear peptide	MAA	Murine MAb LR04
		MDA-LDL	IK17
			Human IgG autoantibodies
			Human IgM autoantibodies
P2	7-mer cyclic peptide	MAA	Murine MAb LR04
		MDA-LDL	IK17
			Human IgG autoantibodies
			Human IgM autoantibodies

significant change in plaque size, as well as in late stages during fibrotic transformation.

Although the nuclear imaging studies described above provided key proof-of-principle evidence that antibodies to OSE can be used to image clinically relevant targets in atherosclerotic lesions, the applied techniques are not easily clinically translatable due to the blood clearance of the antibodies being significantly longer than the half-life of the radioisotope. Longer acting radioisotopes such as ^{64}Copper, ^{89}Zirconium, and ^{111}Indium may be viable alternatives that can be tested in future studies.

MR Imaging Studies

MRI is an optimal alternative to nuclear imaging due to its sub-millimeter resolution, intrinsic tissue contrast and the ability to void the signal of blood by altering the MRI pulse sequences used. Novel molecular imaging probes were designed to deliver high payloads of MR active metals to the molecular targets. The probes were separated into two classes: paramagnetic and superparamagnetic (SPIO) [23, 26, 77].

Despite the class of agent, all molecular imaging agents for MRI must meet the following criteria for clinical translation: (a) *Safety*. The probe must be metabolized or excreted without any safety issues related to the active MRI metal (such as gadolinium (Gd), manganese (Mn), or iron) or the nanoparticle/scaffolding material. (b) *Specificity*. There should be nominal non-specific uptake of the molecular imaging probe. This means that the untargeted material should exhibit limited uptake within the arterial wall of atherosclerotic animals. (c) *Small particle size*. Studies have shown that the nanoparticle must be smaller than the fenestrea of the atherosclerotic vessels. This means that the size of the nanoparticle used to deliver the active MRI metal must be <25 nm, preferably in the range of 5–20 nm [23]. (d) *Pharmacokinetics*. The probes must exhibit some degree of prolonged circulation (half-lives, t1/2, >4 h) to allow for adequate uptake into the arterial wall. However, excessive circulation times (t1/2>24 h) are not desirable either, as they require scanning to be performed at late time points post injection. (e) *Efficacy and payload*. MR signal will be modulated by the payload of the MRI active metal. For paramagnetic materials, typically the larger the number of metal ions associated with the nanoparticle the better the signal modulation. For superparamagnetic materials, the MR signal modulation is directly linked to the size and quality of the iron oxide crystalline core. Table 3 summarizes the advantages and disadvantages of the MRI platforms.

Table 2 Summary of imaging studies targeting oxidation-specific epitopes

Date	Authors	Modality	Label/Dose	Platform	Antibodies	Animal models	Summary of key findings
1999	Tsimikas et al.[15]	Planar/SPECT	^{99}Tc/90 μCi	Direct conjugation	In vivo imaging -MDA2	In vivo imaging −7 WHHL rabbits - 2 NZW rabbits (controls)	MDA2 specifically images atherosclerotic plaques in vivo; First demonstration that oxidation-specific epitopes can be imaged in live animals
			^{125}I		pKa -MDA2 -Halb (control Ab to human albumin)	pKa −7 WHHL and 2 NZW rabbits −5 WHHL and 2 NZW rabbits	
			^{125}I		Biodistribution -MDA2 alone -MDA2 with MDA-LDL	Biodistribution −5 WHHL rabbits -=7 WHHL rabbits	
2001	Tsimikas et al. [16, 18, 20]	Autoradiography	^{125}I	Direct conjugation	In vivo imaging -MDA2 -Halb (control Ab to human albumin)	In vivo imaging −16 WHHL rabbits - 8 NZW rabbits (controls) Progression/Regression study −81 LDLR−/−mice	In vivo uptake of radiolabeled MDA2 provides an accurate measure of atherosclerotic lesions rich in oxidized LDL and is highly sensitive to their regression and plaque stabilization. Autoantibodies to OxLDL correlate with atherosclerosis progression and regression
2008	Briley-Saebo et al. [77]	MRI	Gd/0.075–mol/kg	Micelles	In vivo imaging MDA2 -IK17 -E06 -IgG (control)	In vivo imaging −8 apoE$^{-/-}$ mice −3 apoE$^{-/-}$ mice −8 apoE$^{-/-}$ mice −3 apoE$^{-/-}$ mice	MRI nanoparticles containing Gd-labeled MDA2, IK17, and E06 enhance the aorta of mice with atherosclerosis.
			Gd/0.075–mol/kg		pKa -MDA2 -IK17 -E06 -IgG (control)	pKa - 30 apoE$^{-/-}$ and 14 WT mice	Unlabeled MDA2 competitively inhibits enhancement with Gd-MDA2. Targeted micelles co-localized with macro-phages by confocal imaging.
			Gd/0.075–mol/kg		Biodistribution -MDA2 -IK17 -E06 -IgG (control)	Biodistribution -Total of 30 apoE$^{-/-}$ mice	
2011	Briley-Saebo et al.[23]	MRI	Fe/3.9 mg/kg	Lipid-coated, ultrasmall superparamagnetic iron oxide particles (LUSPIOs)	In vivo imaging -MDA2 -IK17 -E06 -Untargeted (control)	In vivo imaging −8 apoE$^{-/-}$ mice −3 apoE$^{-/-}$ mice −8 apoE$^{-/-}$ mice −8 apoE$^{-/-}$ mice	Specific signal accentuation within the aorta observed following administration of labeled MDA2, IK17, and E06 but not untargeted LUSPIOs.
			Fe/3.9 mg/kg	Lipid-coated, superparamagnetic iron oxide particles (LSPIOs)	In vivo imaging MDA2 IK17 E06 Untargeted (control)	In vivo imaging 8 apoE$^{-/-}$ mice 3 apoE$^{-/-}$ mice 8 apoE$^{-/-}$ mice 8 apoE$^{-/-}$ mice	Signal effect is competitively inhibited by unlabeled MDA2. LUSPIOs co-localize with intra-plaque macrophages, assessed by immunohistochemistry and confocal imaging.

Table 2 (continued)

Date	Authors	Modality	Label/Dose	Platform	Antibodies	Animal models	Summary of key findings
			Fe/3.9 mg/kg		pKa MDA2 IK17 Untargeted (control)	pKa 8–10 apoE$^{-/-}$ and 8–10 WT mice in each group	LSPIOs are too large to enter plaques and cannot image lesion adequately
				LUSPIO and LSPIO			
2012	Briley-Saebo et al. [26]	MRI	Mn/0.050 mol/kg	micelle	In vivo imaging -MDA2 -IK17 -Untargeted (control)	In vivo imaging −8 apoE$^{-/-}$ mice and 8 LDLR$^{-/-}$ mice −8 apoE$^{-/-}$ mice −8 apoE$^{-/-}$ mice and 8 LDLR$^{-/-}$ mice	Labeled OSE antibodies enhance the aorta in both apoE$^{-/-}$ and LDLR$^{-/-}$ mice. MDA2-Mn micelles are located within intra-plaque macrophages on confocal imaging
			Gd/0.050 mol/kg		-MDA2 -Untargeted (control)	−8 apoE$^{-/-}$ mice −8 apoE$^{-/-}$ mice	97 % of MDA2-Mn micelles cleared within 1 week post injection, compared to 72.9 % clearance for MDA2-Gd micelles
			Mn/0.050 mol/kg		pKa -MDA2 -IK17 -Untargeted (control)	pKa −3 apoE$^{-/-}$ and 3 WT mice in each group	
			Mn/0.050 mol/kg		Biodistribution -MDA2 -IK17 -Untargeted (control)	Biodistribution −45 apoE$^{-/-}$ mice (N=3 for each antibody/time point)	
2014	Nguyen et al. [83]	MRI	Mn/0.050 mol/Kg	G8 Dendrimers	In vivo imaging -MDA2 -Untargeted (control)	In vivo imaging −4 apoE$^{-/-}$ mice −3 apoE$^{-/-}$ mice	G8 dendrimers contain a large payload of Mn compared to micelles (768 ions on a dendrimer vs. 50 in a micelle).
					pKa -MDA2 -Untargeted (control)	pKa −3 apoE$^{-/-}$ and 3 WT mice in each group	Mn G8 dendrimers circulate with a half-life of 2.9 h, compared to Mn micelles, which have a half-life of 16.4 h.
					Biodistribution -MDA2 -Untargeted (control)	Biodistribution −18 apoE$^{-/-}$ mice (N=3 for each antibody/time point)	Labeled MDA2, but not untargeted G8 dendrimers enhance the aorta apoE$^{-/-}$ mice on MRI.

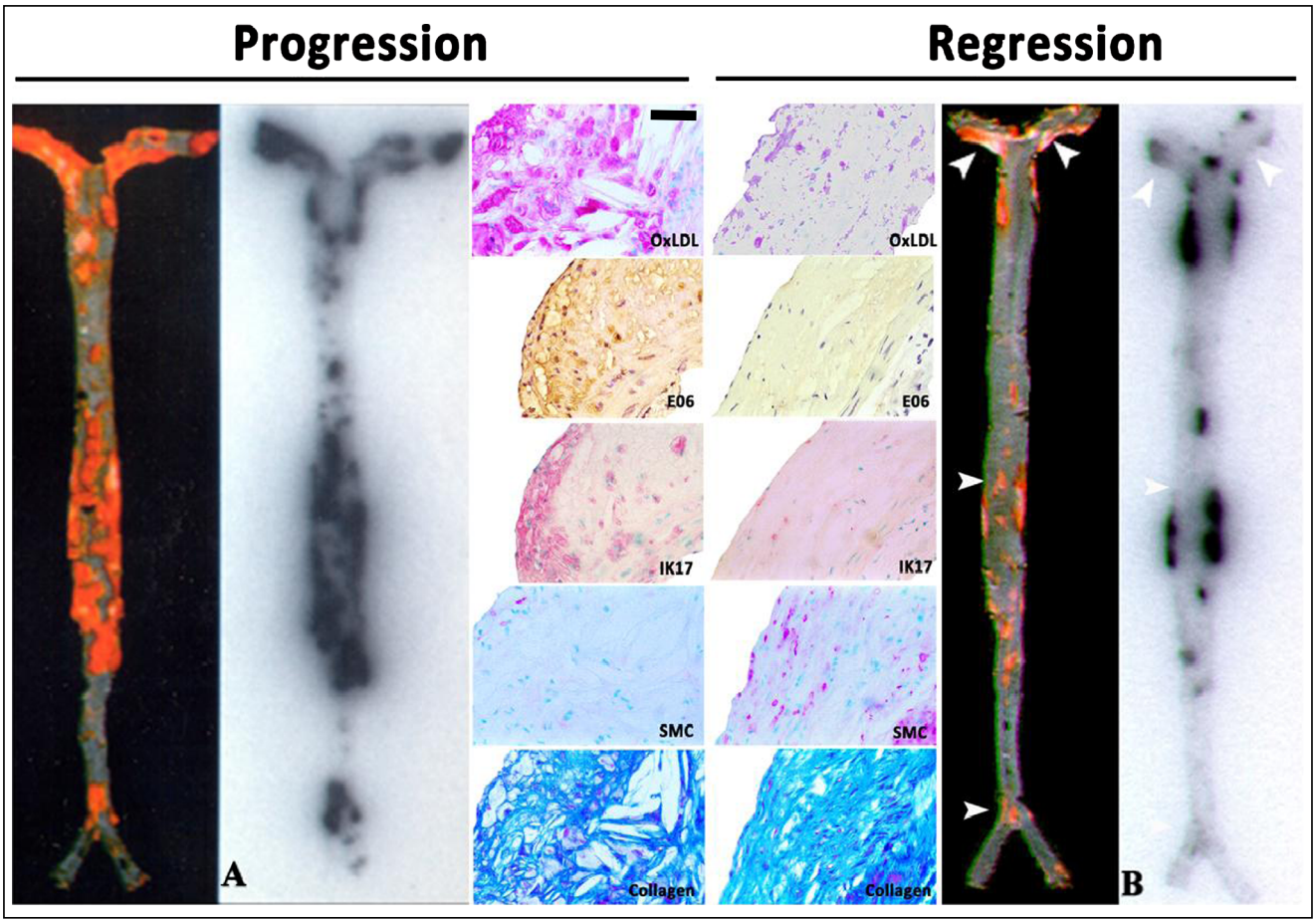

Fig. 3 Autoradiographic and immunohistochemistry representations of ^{125}I-MDA2 accumulation in Sudan stained aortas of LDLR$^{-/-}$ mice undergoing progression and regression diets. Representative en face mouse aortas stained with Sudan red and corresponding autoradiographs of ^{125}I-MDA2 accumulation in mouse aortas following intravenous injection, in Progression (**a**) and Regression (**b**) groups. Representative aortic atherosclerotic lesions from LDLR$^{-/-}$ mice from Progression (*left middle panel*) and Regression (*right middle panel*) groups. Immunostaining for OxLDL, SMCs, and IK17 appear *pink*/*purple*. Collagen is stained with Masson Trichrome and appears *bright blue*. E06 staining appears as *brown* product of peroxidase reaction. Reprinted with permission from Tsimikas et al. [16] and Torzewski et al. [20]. *OxLDL*=oxidized LDL, *SMC*=smooth muscle cells; *bar*=50 μm

Design of MRI Imaging Nanoparticles Composed of Gadolinium and Manganese Micelles and Iron Oxide Nanoparticles for MRI Detection of OSE

Lipid based nanoparticles may allow for the delivery of a high payload of paramagnetic metal ions to the arterial wall, while keeping the total particle size <25 nm. Phospholipids are naturally occurring amphiphilic molecules that contain both a hydrophilic head group and a hydrophobic tail. Amphiphiles self-associate into aggregates and the length of the hydrophobic chains and the size of the head group determine if a micelle like structure (single layer) or a bilayer (liposome) structure is formed. Micelles were generated to contain the following components: PEG-DSPE (1,2-distearoyl-sn-glycer-3-phosphoethanolamine-n-methoxy(polyethylene glycol-2000), Gd or Mn diethylene triamine pentaacetic acid (DTPA)-bis(stearyl-amid) (GdDTPA-BSA or MnDTPA-BSA) and PEG-malamide-DSPE, (molar ration of 49:50:1). Targeted nanoparticles were created by covalently attaching the antibodies (MDA2, E06 or IK17) to the micelles by using SATA modification techniques (Fig. 4) [26, 77]. Table 4 summarizes the characteristics of magnetic resonance nanoparticles targeting OSE.

MR Imaging with Gadolinium Nanoparticles

Gadolinium is the most commonly used paramagnetic metal ion since is the most effective with respect to MR signal enhancement (increase the longitudinal relaxation rate, R1). The Gd nanoparticles exhibited in vitro R1 values that were ×3 greater than GdDTPA (the linear chelate not bound to the nanoparticle) at clinical imaging field strengths [77]. The blood half-life was ≈1.5 h for both targeted and untargeted formulations in wild-type mice following i.v. administration of a 0.075-mmol Gd/kg dose. In cholesterol fed apoE$^{-/-}$ mice, MDA2, IK17, and E06

Table 3 Summary of advantages and disadvantages of the MRI platforms

Platform	Advantages	Disadvantages
Gd Micelles	*Able to detect OSE in the arterial wall of atherosclerotic mice *Positive MR signal enhancement (T1 agent) *Easy and reproducible synthesis	*Toxicity related issues due to bio-retention and bio-transformation *Optimal imaging time point >72 h p.i.
Mn Micelles	*Able to detect OSE in the arterial wall of atherosclerotic mice The agent is a switch, with little or no signal in the vascular phase and strong signal enhancement (T1 agent) in the arterial wall. *No issues related to toxicity as Mn is an endogenous metal ion that is safe when chelated in the bolus phase *Easy and reproducible synthesis	*Non-traditional approach *Optimal imaging time point at 48 h p.i.
Mn Dendrimers	*Able to detect OSE in the arterial wall of atherosclerotic mice *Dendrimers offer a high payload of Mn relative to the micelles (1024 vs. 300 Mn ions/particle). * Positive MR signal enhancement (T1 agent) *No issues related to metal ion toxicity, as Mn, is an endogenous metal that is safe when chelated in the bolus phase.	*Potential safety/toxicity of dendrimers still not established *Blood half-life may be too low for optimal arterial wall imaging (may need PEG in formulation). *Optimal imaging time point at 48 h p.i.
Iron Oxides	*Able to detect OSE in the arterial wall of atherosclerotic mice *Iron oxides have better sensitivity than paramagnetic agents due to their increased magnetic moment (10 times more sensitive). *No issues related to toxicity, as Fe is an endogenous metal ion. *Optimal imaging time point at 24 h p.i.	*Causes MR signal loss (T2* agent). * Iron in the arterial wall may induce oxidation [6, 85].

nanoparticles had consistently prolonged half-life consistent with delayed clearance, possibly due to binding to circulating OSE.

The diagnostic efficacy of the OSE targeted Gd nanoparticles was evaluated over a 3-week time period post injection in apoE$^{-/-}$ mice. To remove the background signal from blood and to allow for delineation of the arterial wall, black blood T1-weighted sequences were used with 16 contiguous 500-μm-thick slices with a microscale in-plane resolution of 101 μm. The percent-normalized enhancement (%NENH) was determined relative to muscle and reflects the percent change in the contrast-to-noise ratios obtained pre and post injection. At 72 h post injection, the OSE targeted nanoparticles demonstrated optimal (highest) MR signal enhancement (125 % to 231 %, depending on the OSE antibody used), relative to adjacent muscle (Fig. 5a shows an example of IK-17-Gd nanoparticles). Consistent with a specific targeting mechanism, pre-injection of antibody MDA2 before intravenous injection of the MDA-targeted nanoparticles resulted in ≈6-fold reduction in %NENH at 72 h post injection. In vitro studies incubating macrophages with OxLDL and MDA2-targeted nanoparticles showed that the nanoparticles accumulated within macrophages, through a mechanism of binding extracellular OxLDL and then the entire complex taken up by macrophages, likely through scavenger receptors. Histology and confocal microscopy (rhodamine label associated with the micelles) shows the high specify of the OSE targeted nanoparticles to intra-plaque macrophages (Fig. 5b). These data show that these micelles not only bind to and image extracelluler OSE, but also accumulate within macrophages, giving them the property of being indirect macrophage imaging agents.

In other studies, co-localization of the targeted Gd micelles with macrophages in atherosclerotic plaques was observed

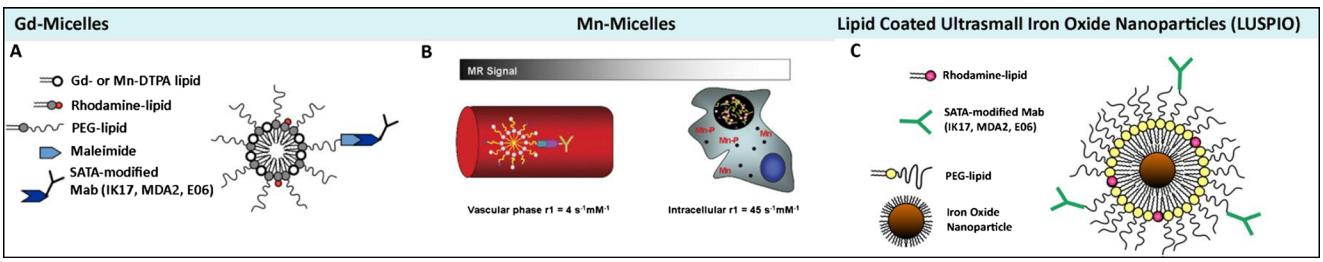

Fig. 4 Design of gadolinium and manganese micelles and lipid-coated ultrasmall iron oxide nanoparticles. *Panel A* is a schematic of Gd-micelles, *panel B* of Mn-micelles, and *panel C* of lipid-coated, ultra small, iron oxide nanoparticles (LUSPIO), all attached to respective SATA modified antibodies. Mn is released with the endosomes/lysosomes after uptake into intraplaque macrophage/foam cells (*black circle*). Due to intracellular release of Mn and subsequent interaction with intracellular components, the magnetic resonance (MR) signal is greatly enhanced. *OSE*=oxidation-specific epitope. Details of synthesis and composition are available in Briley-Saebo et al. [23, 26, 77]. Magnification of *panel C* and 4 are ×4. Reprinted with permission from Briley-Saebo et al. [23, 26, 77]

Table 4 Characteristics of magnetic resonance nanoparticles targeting oxidation-specific epitopes

Formulation	Size (nm)	Relaxivity 60 MHz, 40 °C s-1 mM-1	Blood half-life, h		%ID Liver 24 h p.i. apoE$^{-/-}$mice	Enhancement in the arterial wall at the optimal time point p.i. apoE$^{-/-}$mice	Optimal time point for imaging and dose
			apoE$^{-/-}$mice	WT mice			
Gd Micelles		r1				%NENH, 9.4 T	72 h
MDA2	22±2	9.3	14.3*	1.7	18	125**	0.075 mmol Gd/kg
IK17	16±3	10.5	16.5*	1.8	18	138**	
E06	16±3	10.8	20.1*	1.7	32	231**	
IgG	16±4	10.4	1.4	1.3	18	−0.6	
Untargeted	14±2	11.6	1.5	1.5	12	15	
Mn Micelles		r1				%NENH, 9.4 T	48 h
MDA2	18±3	4.1	16.4*,+	NA	5	141**	0.05 mmol Mn/kg
IK17	12±2	3.8	12.3*,+	NA	5	135**	
E06	NA	NA	NA	NA	NA	NA	
IgG	NA	NA	NA	NA	NA	NA	
untargeted	10±2	4.1	3.4*,+	NA	4	12	
MDA2-intracellular		*45*					
Mn Dendrimers		r1				%NENH, 3 T	48 h
MDA2	13±1	3.5	1.9*	0.9	11	62**	0.05 mmol Mn/kg
IK17	NA	NA	NA	NA	NA	NA	
E06	NA	NA	NA	NA	NA	NA	
IgG	NA	NA	NA	NA	NA	NA	
Untargeted	12±1	3.4	0.8	0.8	1	16	
Iron Oxides		r2				ΔR2*(%), 9.4 T	24 h
MDA2	14±3	37	9.01*	1.55	31	56**	3.9 mg Fe/kg
IK17	12±2	35	9.12	NA	31	58**	
E06	16±4	38	9.32	NA	30	62**	
IgG	NA	NA	NA	NA	NA	NA	
Untargeted	10±3	35	1.52	1.41	25	0.5	

Comparison of the physical and chemical properties of the various OSE targeted formulations. The size represents the mean hydrodynamic diameter as determined by light scattering. The blood half-lives were determined in apoE$^{-/-}$ and background wild type mice following i.v. injection at the specified dose administered (last column of table). The percent injected dose (%ID) in the liver is also shown, 24 h after i.v. injection of the specified dose. The enhancement in the arterial wall is reflected in either the percent normalized enhancement (%ENH) or the percent relative change in R2* at the optimal imaging time p.i. The optimal imaging time was determined based upon when maximum %ENH or deltaR2* values were obtained. The field strength used to obtain the in vivo MR images is also specified. MR imaging for all studies, except the dendrimers, was performed at 9.4 T using a specialized mouse coil. For the dendrimers, imaging was performed using a clinical 3 T system

24 h to 3 weeks post injection of the OSE targeted formulations [26]. The biodistribution data showed significant uptake of the untargeted and OSE targeted Gd micelles in the liver (20–30 % ID at 24 h post injection) and spleen (1–2 % ID). Imaging to >3 weeks showed MR signal enhancement within the arterial wall following administration of the OSE targeted Gd micelles, suggesting transmetallation of the Gd metal ion and the formation of toxic Gd salts [77, 82]. Due to these potential safety issues of Gd accumulation in the liver, Gd is not an ideal MR label for clinical OSE imaging using this approach.

MR Imaging with Manganese Nanoparticles and G8 Dendrimers

Manganese (Mn(II)) is an endogenous paramagnetic metal ion with Food and Drug Administration approval for intracellular imaging. Mn is typically not used as the MR active metal since it has a low magnetic moment, relative to Gd, that limits MR signal enhancement. However, studies have shown that if Mn is delivered into a cell, interaction with intracellular components results in significant (>20-fold) increases in MR efficacy, relative to chelated Mn(II) (such as MnDTPA, MnDPDP, and MnCDTA). As a result, we designed an OSE targeted Mn probe that stays chelated in the vascular phase (with limited biotransformation and de-chelation) and releases the Mn once it is taken up by intra-plaque macrophages. With this approach a switch like probe is created with limited signal in the vascular phase due to the magnetic properties associated with chelated Mn(II) (as MnDTPA) and high MR signal once it reaches its intracellular target as Mn is released from the DTPA chelate and binds to cellular components.

OSE targeted Mn micelles were synthesized, characterized, and tested in pre-clinical models of atherosclerosis [26]. Characterization of the micelles revealed that there were approximately 50 paramagnetic ions per micelle. For the targeted formulations, approximately one out of 30 micelles was conjugated with an antibody. As expected, the in vitro

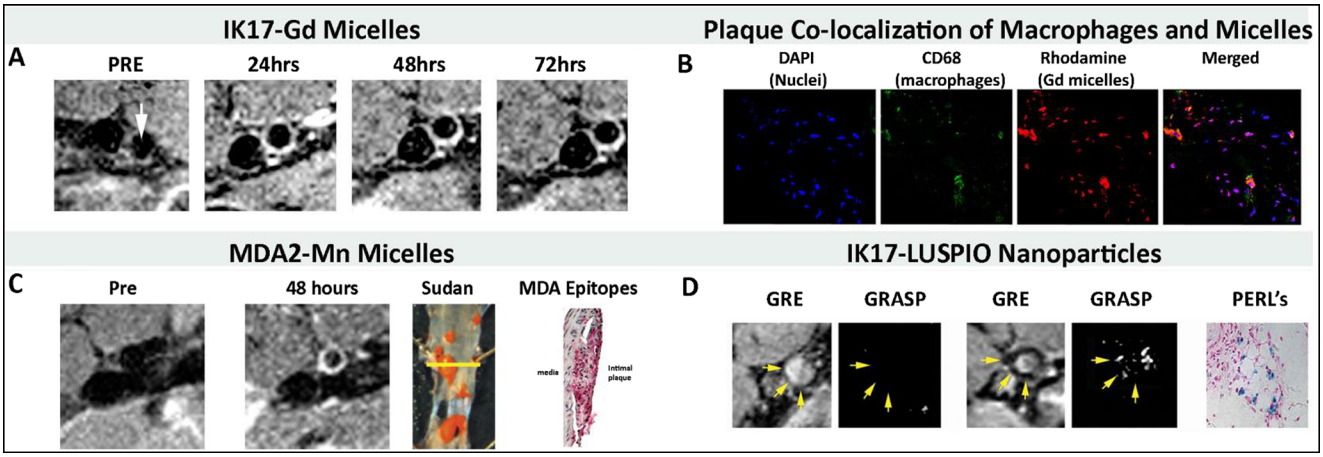

Fig. 5 MR imaging studies and confocal microscopy and immunostaining of mouse atherosclerotic lesions. *Panel C* shows representative non-invasive MRI imaging of abdominal aortas of LDLR$^{-/-}$ mice using IK17-Gd-micelles. There is no signal at the pre-injection scan and maximum signal (*white contrast*) at 48–72 h. *Panel D* shows Confocal microscopy of apoE$^{-/-}$ mouse aortic atherosclerotic plaque after intravenous administration of MDA2 micelles demonstrating nuclei (*blue*), macrophages (*green*), and micelles (*red*). *Panel E* shows non-invasive MRI imaging with Mn-MDA2-micelles with the accompanying panels showing the Sudan (*lipid*) and MDA immunostained aortas. *Panel F* shows non-invasive MRI imaging with IK17-LUSPIO micelles with accompany panel H&E stained apoE$^{-/-}$ mouse aorta with Perl's stain for iron oxide. Iron oxide causes signal loss and it can be seen that the abdominal aorta plaque becomes darker following injection. The gradient echo acquisition for super paramagnetic particles with positive contrast (GRASP) sequence differentiates between iron oxide deposition (now shown as white signal) and artifacts that are often present when imaging the arterial wall. Reprinted with permission from Briley-Saebo et al. [23, 26, 77]

saline and plasma R1 values were 2–3 times less (depending of matrix) than that of the Gd micelles due to the magnetic properties of chelated MnDTPA. Once taken up by macrophages, the R1 of the OSE targeted Mn micelles increased dramatically from 4 s^{-1} mM^{-1} to 45 s^{-1} mM^{-1}. The in vivo biodistribution data showed 97 % clearance of the MDA2-Mn micelles within 1 week post-injection. Significant MR signal enhancement was observed in the arterial wall of atherosclerotic mice following a 0.05 mmol Mn/kg dose of OSE targeted Mn micelles, relative to untargeted formulations (Fig. 5c). To compare the MR efficacy of OSE targeted Mn and Gd micelles, MDA2-Mn micelles were administered at a dose that was 33 % lower than that of Gd but had equivalent MR signal enhancement [26]. For targeted Mn micelles, maximum signal enhancement was observed 48 to 72 h post-injection %NENH=141±20 %), with no significant signal observed after 1 week. MDA2-Gd micelles, however, exhibited maximum enhancement after 1 week post-injection (%NENH=156±21 %). The study clearly demonstrated that OSE targeted Mn micelles allow for the detection of OSE-rich intraplaque macrophages without the safety concerns associated with Gd formulations.

Poly(amido amine) (PAMAM) dendrimers are synthetic macromolecules composed of repeating beta-alanine subunits. The dendrimers are used to load large amounts of Mn while keeping the particle size small enough (<20 nm) to allow for intra-plaque macrophage uptake. Generation eight dendrimers (G8) contain 1024 primary amine groups that may be modified and labeled with MnDTPA, a significant improvement over the MnDTPA micelles where there are≈50 MnDTPA per micelle [83]. The hydrodynamic size (diameter) and in vitro R1 values associated with the OSE targeted dendrimers were similar to the values reported for the targeted Mn micelles (13.34±1.2 nm, R1 saline=3.5 s-1 mM-1). MR images obtained prior to and after the administration of untargeted and OSE targeted dendrimers displayed a maximum arterial wall enhancement at 48 h post injection at 62±3 % (%NENH). Future studies will be performed to evaluate the efficacy of targeted Mn dendrimers and micelles at both 9.4 T and 3 T and determine their relative value in imaging OSE.

MR Imaging with OSE-Targeted, Lipid Coated, Superparamagnetic Iron Oxide Nanoparticles

Lipid coated superparamagnetic iron oxide nanoparticles (LUSPIO) contrast agents are composed of iron oxide crystals (4 nm) and coated with PEG lipids that prevents aggregation of the iron cores [23] and the OSE antibodies attached using the same methods described for the micelles. Unlike the OSE targeted paramagnetic micelles and dendrimers that promote MR signal increase, lipid-coated, LUSPIOs induce proton dephasing that results in MR signal loss. The ability of iron oxide particles to induce MR signal loss is characterized by the properties associated with both the iron oxide core as well as interactions between the crystals due to aggregation or agglomeration. As a result, the MR efficacy is modulated by the magnetization of the iron oxide core at the imaging field strength, the diffusion of water protons in the local magnetic field generated by the LUSPIO, and aggregation or agglomeration of the iron oxide particles. For OSE imaging, intraplaque macrophages will take up the targeted SPIO particles. Compartmentalization within the cells as well as the

possibility for intracellular agglomeration causes significant MR signal loss. The sensitivity of LUSPIOs, relative to similar paramagnetic formulations is roughly 10 times greater due the high magnetization associated with LUSPIOs. Additionally, iron oxide particles are considered safe in that macrophages safely metabolize iron oxide particles within the endosomes and lysosomes associated with the cells. The degraded iron is bound to transferrin or other proteins and is safely eliminated by the cell and enters the endogenous iron pool. The FDA has approved the use of iron oxide particles for MR liver indications (Feridex) as well as for anemia treatment (Ferumoxytol).

OSE targeted LUSPIOs were synthesized, characterized, and the pre-clinical efficacy evaluated (Fig. 5d) [23]. MR Imaging was performed at 9.4-T, using the same system as Gd and Mn nanoparticles, at baseline and 24 h after the administration of a 3.9-mg Fe/kg dose. To obtain in vivo R2* maps, multiple gradient echo (GRE) sequences were generated for the matched pre- and post-images on a pixel-by-pixel basis using a custom Matlab [23]. The R2* values were obtained with regions of interest drawn on the arterial wall on slices and the relative percentage change in the R2* values pre/post were determined. Immediately after GRE acquisition, a gradient echo acquisition for superparamagnetic particles with positive contrast (GRASP) sequence was applied using 50 % of the z-rephasing gradient. The GRASP sequence is useful when trying to determine whether MR signal loss is due to iron oxide deposition or other endogenous artifacts (motion, partial voluming, and peri-vascular effects) that might also promote signal loss. Because equivalent imaging geometry was used for both GRE and GRASP, the imaging results obtained from these sequences were directly matched and compared. ICP-MS, confocal microscopy and Perl's staining confirmed the uptake of the OSE targeted SPIOs in the arterial wall, specifically within intraplaque macrophages/foam cells in atherosclerotic mice. It was clearly demonstrated that OSE targeted SPIOs allowed for in vivo detection of OSE rich atherosclerotic plaques.

For clinical translation, prolonged MR signal enhancement within the arterial wall following administration of the OSE targeted Gd micelles and increased accumulation in the liver suggests the occurrence of transmetallation of the Gd metal ion and the formation of toxic Gd salts, making Gd-micelles less attractive for clinical applications. Mn-micelles have an attractive mechanism of plaque enhancement in that they do not generate contrast in the lesion until taken up by macrophages, making them indirect macrophage imaging agents. This is an attractive property in imaging vulnerable plaques. However, toxicology studies would need to be performed to ensure safety of such a micelle formulation. Finally, iron oxides are already approved for clinical applications. An important advantage of our designed LUSPIO vs. dextran-coated iron oxide particles is that LUSPIO only accumulate in macrophages if LUSPIO contain targeting oxidation-specific Abs, thus, they have unique macrophage specificity compared to non-specific iron oxides [23].

Future Directions—Targeting Ose with Natural Antibodies and Macrophage Scavenger Redeptors on Macrophages with Lipopeptides and Mimotopes

We have recently generated a panel of novel natural antibodies (Nabs) from umbilical cord blood (i.e. the fetus was not exposed to environmental factors) and validated leading NAbs as binding OSE. However, a disadvantage of lipopeptides and mimotopes is that they may have reduced affinity and specificity for OSE and not image as well as NAbs. Therefore, all approaches need to be experimentally tested. Also, these approaches will allow us to determine whether imaging extracellular OSE, as detected by NAbs, is similar, better, or complementary than imaging MSR, as detected by lipopeptides and peptides. Finally, LUSPIO nanoparticles rather than Gd- or Mn-micelles will be used since iron oxides are already approved for clinical applications. An important advantage of our designed LUSPIO vs. dextran-coated iron oxide particles is that LUSPIO only accumulate in macrophages if LUSPIO contain targeting oxidation-specific Abs, thus, they have unique macrophage specificity compared to non-specific iron oxides.

Theoretically, NAbs will be preferable relative to murine/human adaptive antibodies since they represent so-called "germline" VDJ recombinations and are present to some extent in most humans. NAbs would predominantly target extracellular OSE present on OxLDL, modified plaque proteins and apoptotic/necrotic macrophages in the lesion core. Presumably, these would have similar imaging efficacy as shown with murine MAbs, but may be potentially safer in humans as they represent NAbs present since birth.

In addition, as part of the LIPID MAPS collaboration, we have developed lipopeptides that bind specifically to MSRs CD36 and SRA present on activated macrophages that can be developed as molecular imaging probes, such as, Bt-PEG3-TGT-K(POVPC)-GG-OH, a stable analogue of POVPC (Fig. 6a) [84]. This POVPC peptide is bound by both NAb E06 and MSR CD36 with high affinity. It is composed of a hexapeptide with one lysine (K) modified by POVPC, in which the sn2 side chain carbonyl group has been covalently linked to the lysine e-amine to form a stable tertiary amine. The POVPC moiety, which contains the PC headgroup, is the actual ligand for CD36. The short PEG group added prior to biotinylation results in high affinity binding. These lipopeptides may be modified for use with PET or placed on micelles or LUSPIO for imaging activated macrophages.

Mimotopes are small peptides that mimic a given MAb's epitope structurally, but not necessarily by amino acid

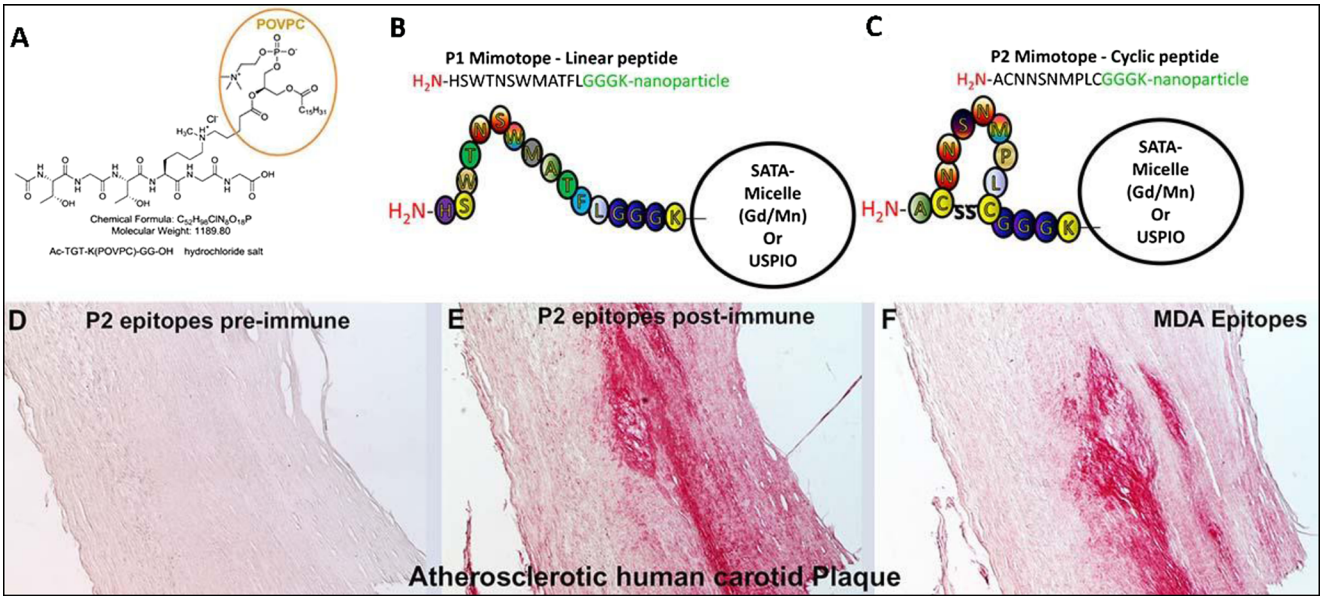

Fig. 6 Structures of lipopeptides and mimotopes. Stable lipopeptides representing an OxPL analogue of POVPC (**a**). Schematic representation of synthesized linear P1 and cyclic P2 peptides mimicking a specific MDA epitope (**b**, **c**). P1 is a linear dodecameric peptide (HSWTNSWMATFL), and P2 is a cyclic heptameric peptide (C NNSNMPL C). The peptides' C terminus containing a GGGC-spacer was amidated. **c** Immunohistochemical staining of human carotid endarterectomy specimens. Sections were stained with pooled preimmune (**d**) or postimmune plasma (**e**) of P2-BSA-immunized mice or with the MDA-LDL-specific MAb MDA2 (**f**). Positive staining is indicated by red color, and nuclei are counterstained with hematoxylin. Magnification is ×4. Reprinted with permission from Turner et al. [84] and Amir et al. [79]

sequence. To clone mimotopes, we utilized a commercial 7–12 amino acid peptide phage display library. These peptide libraries were screened for the ability to bind to the murine IgM NAb LR04, developed in our laboratory, which binds specifically to the MAA epitope [79]. We synthesized peptide P1 from the Ph.D.-12 library (amino acid sequence: HSWTNSWMATFL) (Fig. 6b) and P2 from the Ph.D.7C7 cyclic library (ACNN SNMPLC) (Fig. 6c). Immunization of mice with P2-BSA induced high-titered antisera with specificity for MDA-LDL and MAA-MSA, and those antisera strongly immunostained human carotid endarterectomy plaques (Fig. 6d-f). When used as plated antigens, P1 and P2 detected anti MDA-LDL and anti-MAA antibodies in an analogous manner as did the traditional antigen, MDA-LDL. We have utilized these mimotopes as antigens, and demonstrated that they detected IgG and IgM autoantibodies in sera of healthy subjects and patients undergoing PCI and the titers of autoantibodies changed significantly post PCI and correlated significantly with respective antibody titers against MDA-LDL [79]. These mimotopes may also serve as standardized antigens that will be useful for diagnostic and therapeutic applications in CVD.

As opposed to NAbs that target extracellular OSE and indirectly macrophages through uptake of OSE-Ab complexes, lipopeptides and mimotopes will act as "antigens" and target MSR directly. It is not clear which of these approaches may be more efficacious or preferable for imaging high-risk plaques until further studies are performed. Lipopeptides and mimotopes may each have advantages and disadvantages in human applications. Lipopeptides are attractive as small, OSE-containing molecules that bind MSR with high affinity. OSE mimotopes are small peptides that mimic OSE three-dimensionally and bind MSR. Small molecules would enhance translatability, as lipopeptides would be more cost-effective and potentially even safer than NAbs, and mimotopes even more cost-effective than lipopeptides since their synthesis is straightforward. Disadvantages of lipopeptides include cost of synthesis due to multiple steps in generating stable and soluble ligands. In addition, lipopeptides and mimotopes may have reduced affinity and specificity for OSE.

Conclusion

OSE are present in human atherosclerotic lesions, and are particularly enriched in pathologically defined vulnerable plaques. Development of imaging approaches to target OSE and the macrophages in which they accumulate, and will allow detection of high risk plaques in susceptible patients and provide the tools to allow surveillance following therapeutic interventions.

Acknowledgements Drs. Tsimikas and Witztum are co-inventors of and receive royalties from patents on oxidation-specific antibodies and mimotopes owned by the University of California San Diego. Dr.

Tsimikas holds a dual appointment at the University of California San Diego and as an employee of Isis Pharmaceuticals, Inc. Dr. Witztum has received honoraria for consulting for Isis Pharmaceuticals, Inc., Regulus Therapeutics Inc., and Intercept Pharmaceuticals. All other authors have reported that they have no relationships relevant to the contents of this paper to disclose.

Sources of Funding and Disclosure This study was funded by grants from the National Institutes of Health R01-HL119828, R01-HL093767, P01-HL055798, P01-HL088093, and U54-HL119893 (to Drs. Witztum and Tsimikas).

References

1. Topol, E. J., & Nissen, S. E. (1995). Our preoccupation with coronary luminology. The dissociation between clinical and angiographic findings in ischemic heart disease. *Circulation, 92*, 2333–2342.
2. Stone, G. W., Maehara, A., Lansky, A. J., de Bruyne, B., Cristea, E., Mintz, G. S., Mehran, R., McPherson, J., Farhat, N., Marso, S. P., Parise, H., Templin, B., White, R., Zhang, Z., & Serruys, P. W. (2011). A prospective natural-history study of coronary atherosclerosis. *The New England Journal of Medicine, 364*, 226–235.
3. Witztum, J. L., & Lichtman, A. H. (2014). The influence of innate and adaptive immune responses on atherosclerosis. *Annual Review of Pathology, 9*, 73–102.
4. Lichtman, A. H., Binder, C. J., Tsimikas, S., & Witztum, J. L. (2013). Adaptive immunity in atherogenesis: new insights and therapeutic approaches. *The Journal of Clinical Investigation, 123*, 27–36.
5. Miller, Y. I., Choi, S. H., Wiesner, P., Fang, L., Harkewicz, R., Hartvigsen, K., Boullier, A., Gonen, A., Diehl, C. J., Que, X., Montano, E., Shaw, P. X., Tsimikas, S., Binder, C. J., & Witztum, J. L. (2011). Oxidation-specific epitopes are danger-associated molecular patterns recognized by pattern recognition receptors of innate immunity. *Circulation Research, 108*, 235–248.
6. Tsimikas, S., & Miller, Y. I. (2011). Oxidative modification of lipoproteins: mechanisms, role in inflammation and potential clinical applications in cardiovascular disease. *Current Pharmaceutical Design, 17*, 27–37.
7. Steinberg, D., & Witztum, J. L. (2010). Oxidized low-density lipoprotein and atherosclerosis. *Arteriosclerosis, Thrombosis, and Vascular Biology, 30*, 2311–2316.
8. Navab, M., Ananthramaiah, G. M., Reddy, S. T., Van Lenten, B. J., Ansell, B. J., Fonarow, G. C., Vahabzadeh, K., Hama, S., Hough, G., Kamranpour, N., Berliner, J. A., Lusis, A. J., & Fogelman, A. M. (2004). Thematic review series: the pathogenesis of atherosclerosis: the oxidation hypothesis of atherogenesis: the role of oxidized phospholipids and HDL. *Journal of Lipid Research, 45*, 993–1007.
9. Glass, C. K., & Witztum, J. L. (2001). Atherosclerosis: the road ahead. *Cell, 104*, 503–516.
10. Aikawa, M., Sugiyama, S., Hill, C. C., Voglic, S. J., Rabkin, E., Fukumoto, Y., Schoen, F. J., Witztum, J. L., & Libby, P. (2002). Lipid lowering reduces oxidative stress and endothelial cell activation in rabbit atheroma. *Circulation, 106*, 1390–1396.
11. Palinski, W., Rosenfeld, M. E., Yla-Herttuala, S., Gurtner, G. C., Socher, S. S., Butler, S. W., Parthasarathy, S., Carew, T. E., Steinberg, D., & Witztum, J. L. (1989). Low density lipoprotein undergoes oxidative modification in vivo. *PNAS, 86*, 1372–1376.
12. Yla-Herttuala, S., Palinski, W., Rosenfeld, M. E., Parthasarathy, S., Carew, T. E., Butler, S., Witztum, J. L., & Steinberg, D. (1989). Evidence for the presence of oxidatively modified low density lipoprotein in atherosclerotic lesions of rabbit and man. *The Journal of Clinical Investigation, 84*, 1086–1095.
13. Palinski, W., Yla-Herttuala, S., Rosenfeld, M. E., Butler, S. W., Socher, S. A., Parthasarathy, S., Curtiss, L. K., & Witztum, J. L. (1990). Antisera and monoclonal antibodies specific for epitopes generated during oxidative modification of low density lipoprotein. *Arteriosclerosis, 10*, 325–335.
14. Palinski, W., Horkko, S., Miller, E., Steinbrecher, U. P., Powell, H. C., Curtiss, L. K., & Witztum, J. L. (1996). Cloning of monoclonal autoantibodies to epitopes of oxidized lipoproteins from apolipoprotein E-deficient mice. Demonstration of epitopes of oxidized low density lipoprotein in human plasma. *The Journal of Clinical Investigation, 98*, 800–814.
15. Tsimikas, S., Palinski, W., Halpern, S. E., Yeung, D. W., Curtiss, L. K., & Witztum, J. L. (1999). Radiolabeled MDA2, an oxidation-specific, monoclonal antibody, identifies native atherosclerotic lesions in vivo. *Journal of Nuclear Cardiology, 6*, 41–53.
16. Tsimikas, S., Shortal, B. P., Witztum, J. L., & Palinski, W. (2000). In vivo uptake of radiolabeled MDA2, an oxidation-specific monoclonal antibody, provides an accurate measure of atherosclerotic lesions rich in oxidized LDL and is highly sensitive to their regression. *Arteriosclerosis, Thrombosis, and Vascular Biology, 20*, 689–697.
17. Shaw, P. X., Horkko, S., Chang, M. K., Curtiss, L. K., Palinski, W., Silverman, G. J., & Witztum, J. L. (2000). Natural antibodies with the T15 idiotype may act in atherosclerosis, apoptotic clearance, and protective immunity. *The Journal of Clinical Investigation, 105*, 1731–1740.
18. Tsimikas, S., Palinski, W., & Witztum, J. L. (2001). Circulating autoantibodies to oxidized LDL correlate with arterial accumulation and depletion of oxidized LDL in LDL receptor-deficient mice. *Arteriosclerosis, Thrombosis, and Vascular Biology, 21*, 95–100.
19. Shaw, P. X., Horkko, S., Tsimikas, S., Chang, M. K., Palinski, W., Silverman, G. J., Chen, P. P., & Witztum, J. L. (2001). Human-derived anti-oxidized LDL autoantibody blocks uptake of oxidized LDL by macrophages and localizes to atherosclerotic lesions in vivo. *Arteriosclerosis, Thrombosis, and Vascular Biology, 21*, 1333–1339.
20. Torzewski, M., Shaw, P. X., Han, K. R., Shortal, B., Lackner, K. J., Witztum, J. L., Palinski, W., & Tsimikas, S. (2004). Reduced in vivo aortic uptake of radiolabeled oxidation-specific antibodies reflects changes in plaque composition consistent with plaque stabilization. *Arteriosclerosis, Thrombosis, and Vascular Biology, 24*, 2307–2312.
21. Tsimikas, S., Aikawa, M., Miller, F. J., Jr., Miller, E. R., Torzewski, M., Lentz, S. R., Bergmark, C., Heistad, D. D., Libby, P., & Witztum, J. L. (2007). Increased plasma oxidized phospholipid:apolipoprotein B-100 ratio with concomitant depletion of oxidized phospholipids from atherosclerotic lesions after dietary lipid-lowering: a potential biomarker of early atherosclerosis regression. *Arteriosclerosis, Thrombosis, and Vascular Biology, 27*, 175–181.
22. Tsimikas, S., Miyanohara, A., Hartvigsen, K., Merki, E., Shaw, P. X., Chou, M. Y., Pattison, J., Torzewski, M., Sollors, J., Friedmann, T., Lai, N. C., Hammond, H. K., Getz, G. S., Reardon, C. A., Li, A. C., Banka, C. L., & Witztum, J. L. (2011). Human oxidation-specific antibodies reduce foam cell formation and atherosclerosis progression. *Journal of the American College of Cardiology, 58*, 1715–1727.
23. Briley-Saebo, K. C., Cho, Y. S., Shaw, P. X., Ryu, S. K., Mani, V., Dickson, S., Izadmehr, E., Green, S., Fayad, Z. A., & Tsimikas, S. (2011). Targeted iron oxide particles for in vivo magnetic resonance detection of atherosclerotic lesions with antibodies directed to oxidation-specific epitopes. *Journal of the American College of Cardiology, 57*, 337–347.
24. Fang, L., Green, S. R., Baek, J. S., Lee, S. H., Ellett, F., Deer, E., Lieschke, G. J., Witztum, J. L., Tsimikas, S., & Miller, Y. I. (2011). In vivo visualization and attenuation of oxidized lipid accumulation in hypercholesterolemic zebrafish. *The Journal of Clinical Investigation, 121*, 4861–4869.
25. Vucic, E., Dickson, S. D., Calcagno, C., Rudd, J. H. F., Moshier, E., Hayashi, K., Mounessa, J. S., Roytman, M., Moon, M. J., Lin, J., Tsimikas, S., Fisher, E. A., Nicolay, K., Fuster, V., & Fayad, Z. A. (2011). Pioglitazone modulates vascular inflammation in

atherosclerotic rabbits: noninvasive assessment with FDG-PET-CT and dynamic contrast-enhanced MR imaging. *JACC: Cardiovascular Imaging, 4*, 1100–1109.
26. Briley-Saebo, K. C., Nguyen, T. H., Saeboe, A. M., Cho, Y. S., Ryu, S. K., Volkava, E., Dickson, S., Leibundgut, G., Weisner, P., Green, S., Casanada, F., Miller, Y. I., Shaw, W., Witztum, J. L., Fayad, Z. A., & Tsimikas, S. (2012). In vivo detection of oxidation-specific epitopes in atherosclerotic lesions using biocompatible manganese molecular magnetic imaging probes. *Journal of the American College of Cardiology, 59*, 616–626.
27. van Dijk, R. A., Kolodgie, F., Ravandi, A., Leibundgut, G., Hu, P. P., Prasad, A., Mahmud, E., Dennis, E., Curtiss, L. K., Witztum, J. L., Wasserman, B. A., Otsuka, F., Virmani, R., & Tsimikas, S. (2012). Differential expression of oxidation-specific epitopes and apolipoprotein(a) in progressing and ruptured human coronary and carotid atherosclerotic lesions. *Journal of Lipid Research, 53*, 2773–2790.
28. Vucic, E., Calcagno, C., Dickson, S. D., Rudd, J. H., Hayashi, K., Bucerius, J., Moshier, E., Mounessa, J. S., Roytman, M., Moon, M. J., Lin, J., Ramachandran, S., Tanimoto, T., Brown, K., Kotsuma, M., Tsimikas, S., Fisher, E. A., Nicolay, K., Fuster, V., & Fayad, Z. A. (2012). Regression of inflammation in atherosclerosis by the LXR agonist R211945: a noninvasive assessment and comparison with atorvastatin. *JACC: Cardiovascular Imaging, 5*, 819–828.
29. Purushothaman, K. R., Purushothaman, M., Levy, A. P., Lento, P. A., Evrard, S., Kovacic, J. C., Briley-Saebo, K. C., Tsimikas, S., Witztum, J. L., Krishnan, P., Kini, A., Fayad, Z. A., Fuster, V., Sharma, S. K., & Moreno, P. R. (2012). Increased expression of oxidation-specific epitopes and apoptosis are associated with haptoglobin genotype: possible implications for plaque progression in human atherosclerosis. *Journal of the American College of Cardiology, 60*, 112–119.
30. Choi, S. H., Yin, H., Ravandi, A., Armando, A., Dumlao, D., Kim, J., Almazan, F., Taylor, A. M., McNamara, C. A., Tsimikas, S., Dennis, E. A., Witztum, J. L., & Miller, Y. I. (2013). Polyoxygenated cholesterol ester hydroperoxide activates TLR4 and SYK dependent signaling in macrophages. *PloS One, 8*, e83145.
31. Ravandi, A., Leibundgut, G., Hung, M.Y., Patel, M., Hutchins, P.M., Murphy, R.C., Prasad, A., Mahmud, E., Miller, Y.I., Dennis, E., Witztum, J.L., & Tsimikas, S. (2014). Release and capture of bioactive oxidized phospholipids and oxidized cholesteryl esters during percutaneous coronary and peripheral arterial interventions in humans. *J Am Coll Cardiol* (in press).
32. Bergmark, C., Dewan, A., Orsoni, A., Merki, E., Miller, E. R., Shin, M. J., Binder, C. J., Horkko, S., Krauss, R. M., Chapman, M. J., Witztum, J. L., & Tsimikas, S. (2008). A novel function of lipoprotein [a] as a preferential carrier of oxidized phospholipids in human plasma. *Journal of Lipid Research, 49*, 2230–2239.
33. Leibundgut, G., Scipione, C., Yin, H., Schneider, M., Boffa, M. B., Green, S., Yang, X., Dennis, E. A., Witztum, J. L., Koschinsky, M. L., & Tsimikas, S. (2013). Determinants of binding of oxidized phospholipids on apolipoprotein (a) and lipoprotein (a). *Journal of Lipid Research, 54*, 2815–2830.
34. Tsimikas, S., & Hall, J. H. (2012). Lipoprotein(a) as a potential causal genetic risk factor of cardiovascular disease: a rationale for increased efforts to understand its pathophysiology and develop targeted therapies. *Journal of the American College of Cardiology, 60*, 716–721.
35. Kamstrup, P. R., Tybjaerg-Hansen, A., & Nordestgaard, B. G. (2014). Elevated lipoprotein(a) and risk of aortic valve stenosis in the general population. *Journal of the American College of Cardiology, 63*, 470–477.
36. Thanassoulis, G., Campbell, C. Y., Owens, D. S., Smith, J. G., Smith, A. V., Peloso, G. M., Kerr, K. F., Pechlivanis, S., Budoff, M. J., Harris, T. B., Malhotra, R., O'Brien, K. D., Kamstrup, P. R., Nordestgaard, B. G., Tybjaerg-Hansen, A., Allison, M. A., Aspelund, T., Criqui, M. H., Heckbert, S. R., Hwang, S. J., Liu, Y., Sjogren, M., van der Pals, J., Kalsch, H., Muhleisen, T. W., Nothen, M. M., Cupples, L. A., Caslake, M., Di Angelantonio, E., Danesh, J., Rotter, J. I., Sigurdsson, S., Wong, Q., Erbel, R., Kathiresan, S., Melander, O., Gudnason, V., O'Donnell, C. J., & Post, W. S. (2013). Genetic associations with valvular calcification and aortic stenosis. *The New England Journal of Medicine, 368*, 503–512.
37. Hung, M. Y., Witztum, J. L., & Tsimikas, S. (2014). New therapeutic targets for calcific aortic valve stenosis: the lipoprotein(a)-lipoprotein-associated phospholipase A_2-oxidized phospholipid axis. *Journal of the American College of Cardiology, 63*, 478–480.
38. Binder, C. J., Horkko, S., Dewan, A., Chang, M. K., Kieu, E. P., Goodyear, C. S., Shaw, P. X., Palinski, W., Witztum, J. L., & Silverman, G. J. (2003). Pneumococcal vaccination decreases atherosclerotic lesion formation: molecular mimicry between Streptococcus pneumoniae and oxidized LDL. *Nature Medicine, 9*, 736–743.
39. Lewis, M. J., Malik, T. H., Ehrenstein, M. R., Boyle, J. J., Botto, M., & Haskard, D. O. (2009). Immunoglobulin M is required for protection against atherosclerosis in low-density lipoprotein receptor-deficient mice. *Circulation, 120*, 417–426.
40. Kyaw, T., Tay, C., Krishnamurthi, S., Kanellakis, P., Agrotis, A., Tipping, P., Bobik, A., & Toh, B. H. (2011). B1a B lymphocytes are atheroprotective by secreting natural IgM that increases IgM deposits and reduces necrotic cores in atherosclerotic lesions. *Circulation Research, 109*, 830–U834.
41. Karvonen, J., Paivansalo, M., Kesaniemi, Y. A., & Horkko, S. (2003). Immunoglobulin M type of autoantibodies to oxidized low-density lipoprotein has an inverse relation to carotid artery atherosclerosis. *Circulation, 108*, 2107–2112.
42. Ravandi, A., Boekholdt, S. M., Mallat, Z., Talmud, P. J., Kastelein, J. J., Wareham, N. J., Miller, E. R., Benessiano, J., Tedgui, A., Witztum, J. L., Khaw, K. T., & Tsimikas, S. (2011). Relationship of IgG and IgM autoantibodies and immune complexes to oxidized LDL with markers of oxidation and inflammation and cardiovascular events: results from the EPIC-Norfolk Study. *Journal of Lipid Research, 52*, 1829–1836.
43. Tsimikas, S., Willeit, P., Willeit, J., Santer, P., Mayr, M., Xu, Q., Mayr, A., Witztum, J. L., & Kiechl, S. (2012). Oxidation-specific biomarkers, prospective 15-year cardiovascular and stroke outcomes, and net reclassification of cardiovascular events. *Journal of the American College of Cardiology, 60*, 2218–2229.
44. Osborn, E. A., & Jaffer, F. A. (2013). The advancing clinical impact of molecular imaging in CVD. *JACC. Cardiovascular Imaging, 6*, 1327–1341.
45. Lindner, J., & Sinusas, A. (2013). Molecular imaging in cardiovascular disease: which methods, which diseases? *Journal of Nuclear Cardiology, 20*, 990–1001.
46. Jaffer, F.A., & Verjans, J.W. (2013). Molecular imaging of atherosclerosis: clinical state-of-the-art. *Heart, 100*, (18):1469–77.
47. Quillard, T., & Libby, P. (2012). Molecular imaging of atherosclerosis for improving diagnostic and therapeutic development. *Circulation Research, 111*, 231–244.
48. Hansson, G. K., & Hermansson, A. (2011). The immune system in atherosclerosis. *Nature Immunology, 12*, 204–212.
49. Libby, P., Lichtman, A. H., & Hansson, G. K. (2013). Immune effector mechanisms implicated in atherosclerosis: from mice to humans. *Immunity, 38*, 1092–1104.
50. Greenberg, M. E., Li, X. M., Gugiu, B. G., Gu, X., Qin, J., Salomon, R. G., & Hazen, S. L. (2008). The lipid whisker model of the structure of oxidized cell membranes. *The Journal of Biological Chemistry, 283*, 2385–2396.
51. Berliner, J. A., Leitinger, N., & Tsimikas, S. (2009). The role of oxidized phospholipids in atherosclerosis. *Journal of Lipid Research, 50*(Suppl), S207–S212.
52. Bochkov, V. N., Oskolkova, O. V., Birukov, K. G., Levonen, A. L., Binder, C. J., & Stockl, J. (2010). Generation and biological activities of oxidized phospholipids. *Antioxidants & Redox Signaling, 12*, 1009–1059.

53. Seimon, T. A., Nadolski, M. J., Liao, X., Magallon, J., Nguyen, M., Feric, N. T., Koschinsky, M. L., Harkewicz, R., Witztum, J. L., Tsimikas, S., Golenbock, D., Moore, K. J., & Tabas, I. (2010). Atherogenic lipids and lipoproteins trigger CD36-TLR2-dependent apoptosis in macrophages undergoing endoplasmic reticulum stress. *Cell Metabolism, 12*, 467–482.
54. Piotrowski, J. J., Shah, S., & Alexander, J. J. (1996). Mature human atherosclerotic plaque contains peroxidized phosphatidylcholine as a major lipid peroxide. *Life Sciences, 58*, 735–740.
55. Holvoet, P., Collen, D., & van de Werf, F. (1999). Malondialdehyde-modified LDL as a marker of acute coronary syndromes. *JAMA, 281*, 1718–1721.
56. Ehara, S., Ueda, M., Naruko, T., Haze, K., Itoh, A., Otsuka, M., Komatsu, R., Matsuo, T., Itabe, H., Takano, T., Tsukamoto, Y., Yoshiyama, M., Takeuchi, K., Yoshikawa, J., & Becker, A. E. (2001). Elevated levels of oxidized low density lipoprotein show a positive relationship with the severity of acute coronary syndromes. *Circulation, 103*, 1955–1960.
57. Tsimikas, S., Bergmark, C., Beyer, R. W., Patel, R., Pattison, J., Miller, E., Juliano, J., & Witztum, J. L. (2003). Temporal increases in plasma markers of oxidized low-density lipoprotein strongly reflect the presence of acute coronary syndromes. *Journal of the American College of Cardiology, 41*, 360–370.
58. Palinski, W., Ord, V. A., Plump, A. S., Breslow, J. L., Steinberg, D., & Witztum, J. L. (1994). ApoE-deficient mice are a model of lipoprotein oxidation in atherogenesis. Demonstration of oxidation-specific epitopes in lesions and high titers of autoantibodies to malondialdehyde-lysine in serum. *Arteriosclerosis and Thrombosis, 14*, 605–616.
59. Palinski, W., Tangirala, R. K., Miller, E., Young, S. G., & Witztum, J. L. (1995). Increased autoantibody titers against epitopes of oxidized LDL in LDL receptor-deficient mice with increased atherosclerosis. *Arteriosclerosis, Thrombosis, and Vascular Biology, 15*, 1569–1576.
60. Weismann, D., Hartvigsen, K., Lauer, N., Bennett, K. L., Scholl, H. P., Charbel Issa, P., Cano, M., Brandstatter, H., Tsimikas, S., Skerka, C., Superti-Furga, G., Handa, J. T., Zipfel, P. F., Witztum, J. L., & Binder, C. J. (2011). Complement factor H binds malondialdehyde epitopes and protects from oxidative stress. *Nature, 478*, 76–81.
61. Chang, M. K., Binder, C. J., Torzewski, M., & Witztum, J. L. (2002). C-reactive protein binds to both oxidized LDL and apoptotic cells through recognition of a common ligand: phosphorylcholine of oxidized phospholipids. *PNAS, 99*, 13043–13048.
62. Chou, M. Y., Fogelstrand, L., Hartvigsen, K., Hansen, L. F., Woelkers, D., Shaw, P. X., Choi, J., Perkmann, T., Backhed, F., Miller, Y. I., Horkko, S., Corr, M., Witztum, J. L., & Binder, C. J. (2009). Oxidation-specific epitopes are dominant targets of innate natural antibodies in mice and humans. *The Journal of Clinical Research, 119*, 1335–1349.
63. Chang, M. K., Binder, C. J., Miller, Y. I., Subbanagounder, G., Silverman, G. J., Berliner, J. A., & Witztum, J. L. (2004). Apoptotic cells with oxidation-specific epitopes are immunogenic and proinflammatory. *The Journal of Experimental Medicine, 200*, 1359–1370.
64. Moore, K. J., & Tabas, I. (2011). Macrophages in the pathogenesis of atherosclerosis. *Cell, 145*, 341–355.
65. Yla-Herttuala, S., Palinski, W., Butler, S. W., Picard, S., Steinberg, D., & Witztum, J. L. (1994). Rabbit and human atherosclerotic lesions contain IgG that recognizes epitopes of oxidized LDL. *Arteriosclerosis and Thrombosis, 14*, 32–40.
66. Rosenfeld, M. E., Palinski, W., Yla-Herttuala, S., Butler, S., & Witztum, J. L. (1990). Distribution of oxidation specific lipid-protein adducts and apolipoprotein B in atherosclerotic lesions of varying severity from WHHL rabbits. *Arteriosclerosis, 10*, 336–349.
67. Yla-Herttuala, S., Palinski, W., Rosenfeld, M. E., Steinberg, D., & Witztum, J. L. (1990). Lipoproteins in normal and atherosclerotic aorta. *European History Journal, 11*(Suppl E), 88–99.
68. Horkko, S., Bird, D. A., Miller, E., Itabe, H., Leitinger, N., Subbanagounder, G., Berliner, J. A., Friedman, P., Dennis, E. A., Curtiss, L. K., Palinski, W., & Witztum, J. L. (1999). Monoclonal autoantibodies specific for oxidized phospholipids or oxidized phospholipid-protein adducts inhibit macrophage uptake of oxidized low-density lipoproteins. *The Journal of Clinical Investigation, 103*, 117–128.
69. Leibundgut, G., Witztum, J. L., & Tsimikas, S. (2013). Oxidation-specific epitopes and immunological responses: translational biotheranostic implications for atherosclerosis. *Current Opinion in Pharmacology, 13*, 168–179.
70. Miller, Y. I., & Tsimikas, S. (2013). Oxidation-specific epitopes as targets for biotheranostic applications in humans: biomarkers, molecular imaging and therapeutics. *Current Opinion in Lipidology, 24*, 426–437.
71. Taleb, A., Witztum, J. L., & Tsimikas, S. (2011). Oxidized phospholipids on apolipoprotein B-100 (OxPL/apoB) containing lipoproteins: a biomarker predicting cardiovascular disease and cardiovascular events. *Biomarkers Medecine, 5*, 673–694.
72. Tsimikas, S., Lau, H. K., Han, K. R., Shortal, B., Miller, E. R., Segev, A., Curtiss, L. K., Witztum, J. L., & Strauss, B. H. (2004). Percutaneous coronary intervention results in acute increases in oxidized phospholipids and lipoprotein(a): short-term and long-term immunologic responses to oxidized low-density lipoprotein. *Circulation, 109*, 3164–3170.
73. Tsimikas, S., Kiechl, S., Willeit, J., Mayr, M., Miller, E. R., Kronenberg, F., Xu, Q., Bergmark, C., Weger, S., Oberhollenzer, F., & Witztum, J. L. (2006). Oxidized phospholipids predict the presence and progression of carotid and femoral atherosclerosis and symptomatic cardiovascular disease: five-year prospective results from the Bruneck study. *Journal of the American College of Cardiology, 47*, 2219–2228.
74. Tsimikas, S., Brilakis, E. S., Miller, E. R., McConnell, J. P., Lennon, R. J., Kornman, K. S., Witztum, J. L., & Berger, P. B. (2005). Oxidized phospholipids, Lp(a) lipoprotein, and coronary artery disease. *The New England Journal of Medicine, 353*, 46–57.
75. Kiechl, S., Willeit, J., Mayr, M., Viehweider, B., Oberhollenzer, M., Kronenberg, F., Wiedermann, C. J., Oberthaler, S., Xu, Q., Witztum, J. L., & Tsimikas, S. (2007). Oxidized phospholipids, lipoprotein(a), lipoprotein-associated phospholipase A2 activity, and 10-year cardiovascular outcomes: prospective results from the Bruneck study. *Arteriosclerosis, Thrombosis, and Vascular Biology, 27*, 1788–1795.
76. Tsimikas, S., Mallat, Z., Talmud, P. J., Kastelein, J. J., Wareham, N. J., Sandhu, M. S., Miller, E. R., Benessiano, J., Tedgui, A., Witztum, J. L., Khaw, K. T., & Boekholdt, S. M. (2010). Oxidation-specific biomarkers, lipoprotein(a), and risk of fatal and nonfatal coronary events. *Journal of the American College of Cardiology, 56*, 946–955.
77. Briley-Saebo, K. C., Shaw, P. X., Mulder, W. J., Choi, S. H., Vucic, E., Aguinaldo, J. G., Witztum, J. L., Fuster, V., Tsimikas, S., & Fayad, Z. A. (2008). Targeted molecular probes for imaging atherosclerotic lesions with magnetic resonance using antibodies that recognize oxidation-specific epitopes. *Circulation, 117*, 3206–3215.
78. Friedman, P., Horkko, S., Steinberg, D., Witztum, J. L., & Dennis, E. A. (2002). Correlation of antiphospholipid antibody recognition with the structure of synthetic oxidized phospholipids. Importance of Schiff base formation and aldol condensation. *The Journal of Biological Chemistry, 277*, 7010–7020.
79. Amir, S., Hartvigsen, K., Gonen, A., Leibundgut, G., Que, X., Jensen-Jarolim, E., Wagner, O., Tsimikas, S., Witztum, J. L., & Binder, C. J. (2012). Peptide mimotopes of malondialdehyde epitopes for clinical applications in cardiovascular disease. *Journal of Lipid Research, 53*, 1316–1326.
80. Crisby, M., Nordin-Fredriksson, G., Shah, P. K., Yano, J., Zhu, J., & Nilsson, J. (2001). Pravastatin treatment increases collagen content and decreases lipid content, inflammation, metalloproteinases, and cell death in human carotid plaques:

implications for plaque stabilization. *Circulation, 103*, 926–933.

81. Mintz, G. S., Pichard, A. D., Popma, J. J., Kent, K. M., Satler, L. F., Bucher, T. A., & Leon, M. B. (1997). Determinants and correlates of target lesion calcium in coronary artery disease: a clinical, angiographic and intravascular ultrasound study. *Journal of the American College of Cardiology, 29*, 268–274.
82. Briley-Saebo, K. C., Geninatti-Crich, S., Cormode, D. P., Barazza, A., Mulder, W. J., Chen, W., Giovenzana, G. B., Fisher, E. A., Aime, S., & Fayad, Z. A. (2009). High-relaxivity gadolinium-modified high-density lipoproteins as magnetic resonance imaging contrast agents. *The Journal of Physical Chemistry. B, 113*, 6283–6289.
83. Nguyen, T. H., Bryant, H., Shapsa, A., Street, H., Mani, V., Fayad, Z. A., Frank, J. A., Tsimikas, S., & Briley-Saebo, K. C. (2014). Manganese G8 dendrimers targeted to oxidation-specific epitopes: In vivo MR imaging of atherosclerosis. *J Magn Reson Imaging*. doi:10.1002/jmri.24606.
84. Turner, W. W., Hartvigsen, K., Boullier, A., Montano, E. N., Witztum, J. L., & Vannieuwenhze, M. S. (2012). Design and synthesis of a stable oxidized phospholipid mimic with specific binding recognition for macrophage scavenger receptors. *Journal of Medicinal Chemistry, 55*, 8178–8182.
85. Briley-Saebo, K. C., Johansson, L. O., Hustvedt, S. O., Haldorsen, A. G., Bjornerud, A., Fayad, Z. A., & Ahlstrom, H. K. (2006). Clearance of iron oxide particles in rat liver: effect of hydrated particle size and coating material on liver metabolism. *Investigative Radiology, 41*, 560–571.